*****This Document is Under Minor Revision and Formatting *****
Tiako P.F. (ed) *Competitive Tools, Techniques, and Methods*. Chronicle of Computing. OkIP. CEST24#20
 https://doi.org/10.55432/978-1-6692-0007-9_10

Power Quality Improvement of a Standalone Power Supply System Powered by PV, Wind, and Batteries via LSTM-based ANN Controllers

Reagan Jean Jacques Molu[1*], molureagan@yahoo.fr
Wulfran Fendzi Mbasso[1], fendzi.wulfran@yahoo.fr
Serge Raoul Dzonde Naoussi[1], sdzonde@gmail.com
Patrice Wira[2], patrice.wira@uha.fr
Harrison Ambe [3], ambe.harrison@ubuea.com
Kenfack Tsobze Saatong[1,4] , saakenft@yahoo.fr

[1]Technology and Applied Sciences Laboratory, U.I.T. of Douala, P.O. Box 8689 – Douala, University of Douala, Cameroon.
[2] IRIMAS Laboratory, University of Haute Alsace, 61 Rue Albert Camus, Mulhouse, 68200, France.
[3] Department of Electrical and Electronics Engineering, College of Technology (COT), University of Buea, P.O. Box Buea 63.
[4] Unité de Recherche d'Automatique et d'Informatique Appliquée, I.U.T. Fotso Victor, P.O. Box 134 – Bandjoun, University of Dschang, Cameroon.

(*) Corresponding author : Reagan Jean Jacques Molu; E-mail : molureagan@yahoo.fr

Abstract: **Standalone electric power supply systems that integrate wind and photovoltaic (PV) technologies are widely employed in various applications. These systems require a battery storage system to ensure a continuous power supply, regardless of changes in loads, wind speed, and solar irradiance. To ensure a reliable and uniform power supply, several modifications need to be implemented in these hybrid systems. Power quality is an essential parameter in autonomous power systems, especially those that depend on hybrid energy sources. The battery should undergo the process of charging when there is an excess of energy and discharging when there is a demand from the loads. To achieve this, a bidirectional power flow circuit is utilized to establish a connection between the battery and the network, incorporating an appropriate controlling mechanism. Even in scenarios where there is only partial shading, a Modified Invasive Weed Optimization technique is employed to achieve the most efficient power operation of the photovoltaic (PV) system. Additionally, a Sliding Mode Control strategy is utilized for the wind turbine. This research investigates the application of multiple photovoltaic (PV) systems and wind turbines, each configured with different arrangements of parallel and series combinations of PV panels. The goal is to determine the appropriate rating for the power supply system. The control units in this hybrid standalone power system utilize artificial neural network (ANN) controllers that are based on long short-term memory (LSTM). The aforementioned controllers, when combined with the proposed control methodologies, improve power quality in various scenarios. The results of this investigation are presented using Hardware-in-the-Loop (HIL) on the OPAL-RT platform to evaluate the efficacy of the proposed methodology.**

Keywords: Standalone electric power supply, Wind and photovoltaic technologies, MPPT, MIWO, Battery storage system, SMC, Power Quality.

I. INTRODUCTION

Renewable energy sources, such as solar and wind power, are increasingly being employed in autonomous power supply systems to mitigate environmental pollution. The integration of a greater proportion of renewable sources can enhance the reliability of the system. Deploying wind and solar energy for electricity generation is the most efficient approach to facilitate the advancement of an environmentally sustainable ecosystem. Typically, the process of converting solar energy into electrical energy involves the use of photovoltaic (PV) modules. On the other hand, wind turbines are utilized to harness mechanical power generated by the movement of wind. Permanent magnet synchronous generators (PMSGs) are employed to convert mechanical energy into electrical power in applications with moderate power demands. As a result, there is an increasing worldwide need for on-site hybrid PV-Wind energy-based standalone power supply systems. The incorporation of a Permanent Magnet Synchronous Generator (PMSG)-based wind and Photovoltaic (PV) systems integration can enhance the reliability of the overall system. However, it is essential to include an energy storage system in standalone setups. It is imperative to maintain power equilibrium and provide consistent power to end-users, particularly when there are fluctuations in wind velocity, solar radiation, and electrical demand. Among a variety of energy storage devices, batteries are commonly considered the most suitable option due to their outstanding performance in terms of both charging and discharging speed. Therefore, this document includes the integration of a battery bank to enhance the dependability and consistency of the system under different operational circumstances. Furthermore, a DC-to-DC bidirectional circuit is utilized to regulate the discharging/charging process of batteries, while considering the power imbalance within the system.

Presented at The 2024 OkIP International Conference on Energy and Sustainable Technologies (CEST) in Oklahoma City, Oklahoma, USA, and Online, on April 3, 2024

To enhance the efficiency of wind turbines and PV panels, the utilization of maximum power point tracking (MPPT) converters and suitable algorithms [5-7] is crucial. The boost converters are integrated into the hybrid standalone power generation system to function as Maximum Power Point Tracking (MPPT) converters. Partial Shading Conditions (PSCs) are a frequently observed occurrence in photovoltaic (PV) systems. Consequently, the research paper integrates the Modified Invasive Optimization (MIWO) algorithm into the Maximum Power Point Tracking (MPPT) converters of each Photovoltaic (PV) system. Similarly, the Sliding Mode Control (SMC) technique is employed to function as the Maximum Power Point Tracking (MPPT) algorithm for each wind turbine. The balance between load power and production is attained by regulating the voltage at the direct current (DC) bus with the help of a bidirectional power flow circuit. In order to ensure the proper functioning of alternating current (AC) loads, it is essential to utilize an inverter that is equipped with a suitable control mechanism. Furthermore, the distribution system functions by delivering power to individual phase loads, which can lead to the existence of unbalanced voltages at the three phase terminals [4, 7]. The excess power is stored in batteries; therefore, it is crucial to maintain a lower battery voltage compared to the voltage at the direct current (dc) bus in order to improve the charging process and achieve maximum efficiency. Similarly, in the case of inadequate power supply from the power generation source, the utilization of batteries becomes essential to supply additional power and fulfill the escalated demand. Hence, it is imperative to integrate a boost operation into the battery discharge procedure.

Fluctuations in voltage within the direct current (dc) link can arise as a result of imbalances in power between the generation and load sources [7]. The control system of the bidirectional power flow circuit is engineered to ensure power equilibrium by leveraging the battery to offset any power disparities. Once the direct current (DC) voltage has been regulated, the inverter can effectively manage and sustain the voltage at the alternating current (AC) bus. However, it is important to effectively manage the inverter to ensure the delivery of high-quality power to the load bus, as end-users consistently have high expectations for superior quality electrical supply. Ensuring the maintenance of stable alternating current (AC) voltages at the point of common coupling (PCC) is crucial, even in scenarios involving unbalanced load operations, sudden load changes, and unpredictable variations in irradiance and wind speed.

Usually, traditional proportional-integral (PI) controllers encounter difficulties in efficiently handling sudden changes in the power system because of their fixed gain design. Therefore, the use of ANN (Artificial Neural Network) based controllers is essential in the development of control techniques for converters in standalone systems. Nevertheless, the application of LSTM: Long Short-Term Memory based Artificial Neural Network (ANN) systems can offer improved responses within a shorter duration, especially when dealing with unfamiliar interference signals. Consequently, a Long Short-Term Memory (LSTM) based deep learning algorithm has been devised for the purpose of constructing Artificial Neural Network (ANN) controllers capable of regulating the voltages at the Direct Current (DC) bus and Alternating Current (AC) bus in various converters. The artificial neural network (ANN) controllers that have been designed are then implemented in the control techniques.

The document is structured according to the following format: Section-II provides a comprehensive and detailed explanation of the system. In Section-III, the paper presents an analysis of the control strategies that utilize Long Short-Term Memory (LSTM) based Artificial Neural Network (ANN) controllers. Section-IV showcases the diverse results obtained by utilizing MATLAB and HIL package. The conclusion can be located in Section-V, accompanied by supplementary system ratings presented in the appendix.

II. System Description

A single wind turbine and photovoltaic (PV) units are insufficient in generating the necessary power with a consistent voltage output for a prolonged period of time. To address this issue, it is imperative to arrange the photovoltaic (PV) modules in a configuration that incorporates a combination of series and parallel connections. This will guarantee that the photovoltaic (PV) unit maintains an adequate voltage and power rating. Each wind turbine is equipped with a Permanent Magnet Synchronous Generator (PMSG) system for the purpose of generating electricity. The electrical power generated by the Permanent Magnet Synchronous Generator (PMSG) is converted from alternating current (AC) to direct current (DC) through the utilization of a diode rectifier. Subsequently, a boost circuit, integrated with an appropriate control algorithm, is interconnected with the wind system to establish a common DC-bus. The number of wind systems required is determined by the power rating specifications. The appendix contains detailed information regarding a standalone wind system and a photovoltaic (PV) module. Each photovoltaic (PV) array is outfitted with a dedicated Maximum Power Point Tracking (MPPT) device to maximize the energy output. In a similar manner, every wind system is outfitted with its own Maximum Power Point Tracking (MPPT) converters. A battery bank is interconnected with the DC-bus via a bidirectional power flow circuit for the purpose of voltage regulation and stabilization. Through the implementation of individual connections between each Maximum Power Point Tracking (MPPT) converter and the Direct Current (DC) link using their respective control methods, these converters collaborate to effectively capture the highest possible amount of energy, regardless of fluctuations in wind speed and solar radiation. The configuration enables the bidirectional circuit to regulate the voltage at the dc-bus.

Tiako P.F. (ed) *Competitive Tools, Techniques, and Methods*. Chronicle of Computing. OkIP. CEST24#20
 https://doi.org/10.55432/978-1-6692-0007-9_10

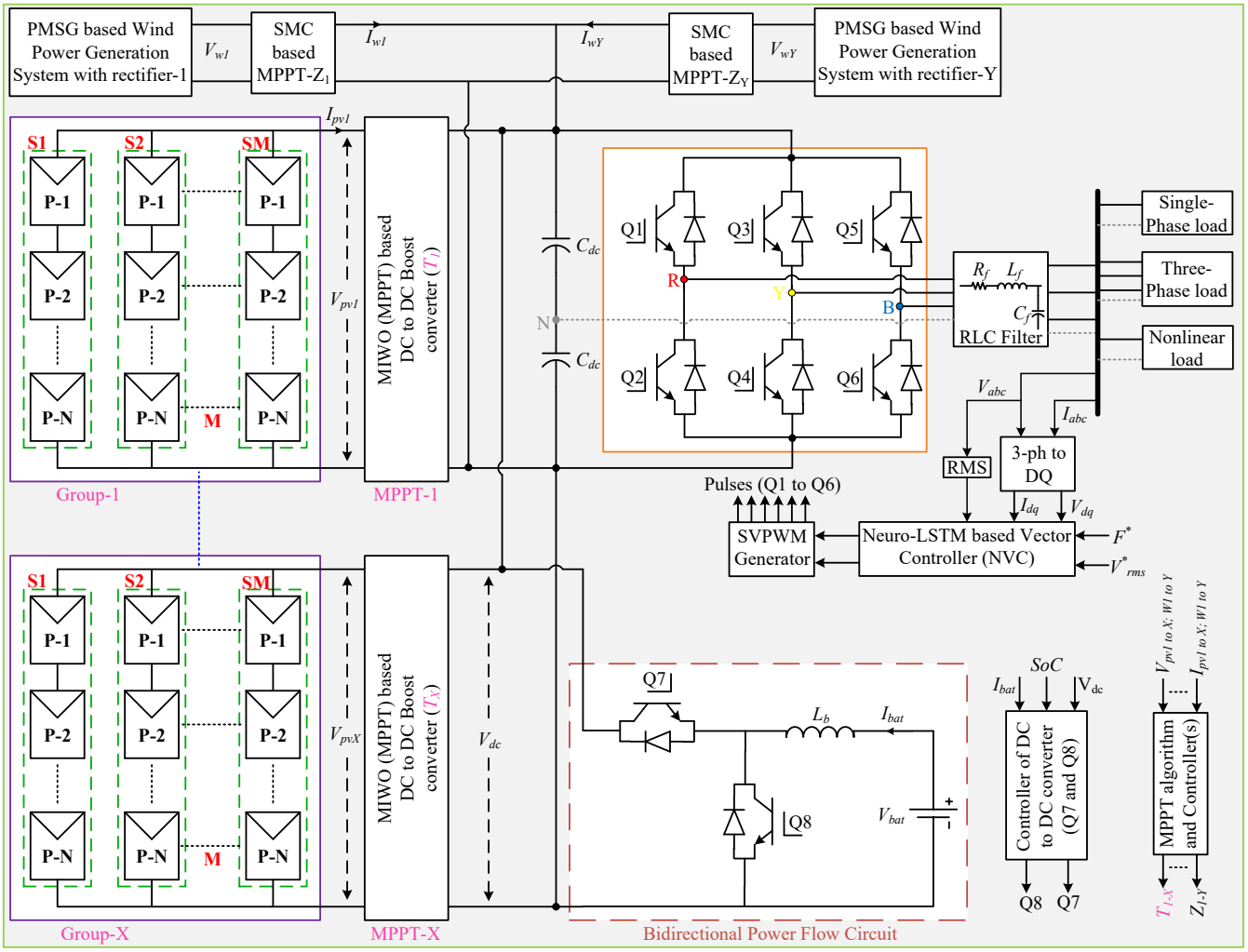

Figure 1: Hybrid standalone system.

An inverter is employed to convert direct current (DC) electrical power into alternating current (AC) electrical power in order to provide power to AC loads. An electrical filter is strategically placed between the point of common coupling (PCC) and the inverter. A 4-wire system is utilized to facilitate the operation of single and three-phase loads exhibiting non-linear characteristics. The schematic depicting the arrangement of a self-contained hybrid battery-wind-photovoltaic (PV) power supply system is shown in Figure 1. The technical specifications of the wind turbine, Permanent Magnet Synchronous Generator (PMSG), batteries, Photovoltaic (PV) module, and filters are derived from prior research. Multiple empirical studies have been conducted by researchers in various experimental conditions, with a selection of them being cited in this specific section. For this particular case, a research study was conducted to deploy an autonomous power supply system that utilized a hybrid configuration of photovoltaic (PV) panels, wind turbines, and energy storage batteries. A research study was conducted to analyze the most effective positioning of an energy management system. A novel Maximum Power Point Tracking (MPPT) methodology was developed for Photovoltaic (PV) systems operating in the presence of partial shading. This approach was developed as part of an independent research investigation. Although a previous study [4] presented a photovoltaic (PV)-based autonomous microgrid, it did not incorporate a wind system. A separate study [8] presented a control methodology that utilizes TS-Fuzzy for a hybrid Diesel-PV system. However, the integration of a diesel generator raised concerns regarding its impact on the environment. The study described in reference [9] introduced an innovative control methodology for a hybrid photovoltaic (PV) powered supply system aimed at achieving voltage regulation. In a separate study, a photovoltaic (PV)-based system utilized double loop proportional-integral (PI) controllers for the direct current (DC)-to-DC converter [10]. A comparative analysis was conducted by a separate group of researchers [11] to assess and evaluate the efficacy of nonlinear controllers in autonomous photovoltaic (PV) systems. Nevertheless, the omission of diverse power generation systems for establishing a unified direct current (DC) connection and the choice to forgo the utilization of artificial neural network (ANN) controllers that rely on long short-term memory (LSTM) were not taken into account. In general, when a nonlinear load is connected to the Point of Common Coupling (PCC), it can produce harmonics that have an impact on other loads. In order to resolve this problem, it is essential to implement an active power filter in conjunction with a DSTATCOM (Distribution Static Synchronous

Compensator) to counterbalance the reactive power requirements imposed by the loads. Furthermore, the researchers have conducted a comprehensive study on the deployment of a microgrid, considering multiple renewable energy sources.

III. Control of Voltage at DC-link and Inverter

Photovoltaic (PV) arrays experience non-uniform solar irradiance, leading to voltage variations at the output terminals of Maximum Power Point Tracking (MPPT) converters. Likewise, wind turbines are unable to function at identical wind velocities. In order to tackle this issue, it is possible to utilize boost converter type MPPT (Maximum Power Point Tracking) converters for the purpose of establishing a shared direct current (dc) link through the integration of all MPPTs. Nevertheless, the direct current (DC) voltage is regulated through a DC-to-DC circuitry, which oversees the operation of charging and discharging the batteries. In scenarios characterized by dynamic system behavior, artificial neural network (ANN) controllers typically exhibit higher performance compared to proportional-integral (PI) controllers. Thus, this document introduces Long Short-Term Memory (LSTM) based Artificial Neural Network (ANN) controllers for the regulation of voltages at the Direct Current (DC) and Alternating Current (AC) bus. Moreover, the weights of the Artificial Neural Network (ANN) are updated using a deep learning algorithm. The Long Short-Term Memory (LSTM) model is depicted in Figure 2, whereas the intricate structure of the LSTM-based Artificial Neural Network (ANN) controller is showcased in Figure 3.

$$a_t = \sigma(b_a + h_{t-1} \times w_{ah} + X_t \times w_{ax}) \quad (1)$$

$$f_t = \sigma(b_f + h_{t-1} \times w_{fh} + X_t \times w_{fx}) \quad (2)$$

$$O_t = \sigma(b_o + X_t \times w_{ox} + h_{t-1} \times w_{oh}) \quad (3)$$

$$\hat{C}_t = \tanh(b_c + X_t \times w_{cx} + h_{t-1} \times w_{ch}) \quad (4)$$

$$s_t = f_t \otimes s_{t-1} + \hat{C}_t \times a_t \quad (5)$$

$$h_t = \tanh(s_t) \otimes O_t \quad (6)$$

The AC bus is susceptible to single-phase power consumption and non-linear loads. These specific loads have the capacity to cause an asymmetry in the three phases of the system, leading to the emergence of '2ω' frequency oscillations in the dc-link voltage. The presence of oscillations can lead to the generation of vibrations in wind turbines and the generation of heat at the terminals of PV panels. To mitigate the impact of these oscillations in the DC-link, a suggested control methodology entails diverting the oscillations through a DC-to-DC circuit and battery. The control mechanism for the DC-to-DC converter is illustrated in Figure 4.

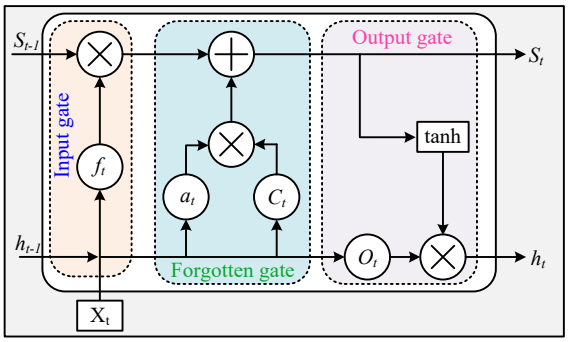

Figure 2: LSTM layout with memory cell.

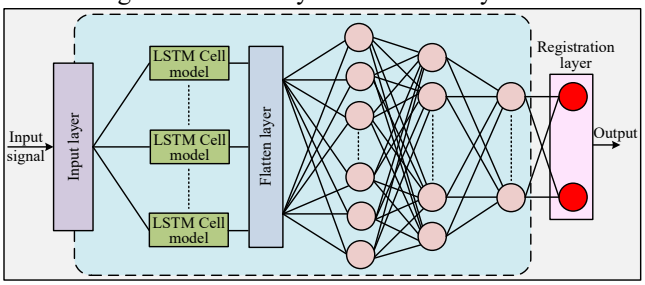

Figure 3: ANN-LSTM controller.

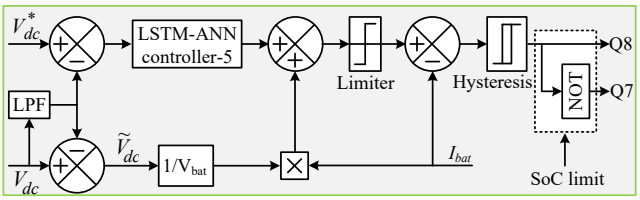

Figure 4: Control scheme of DC-to-DC circuit.

Fluctuations in the direct current (DC) bus voltage can occur as a result of changes in the generated power and the consumed power. The control algorithm for the DC-to-DC converter is designed to maximize the efficiency of using a constant reference signal for the DC-bus voltage. Within the context of Figure 4, the voltage is subjected to a comparison with its corresponding reference signal using a controller that is based on the Long Short-Term Memory (LSTM) Artificial Neural Network (ANN) architecture. The AC component with a frequency of '2ω' in the DC voltage is attenuated by a low pass filter (LPF) and removed from the DC-bus using the recommended control technique. The required pulses are generated by performing a comparison between the reference battery current and the actual battery current using a hysteresis loop. This control methodology enables the transmission of the '2ω' component throughout the DC-to-DC circuit. Moreover, the control scheme additionally integrates the state of charge (SOC) to safeguard the battery against excessive charging and discharging. An inverter, equipped with a suitable control algorithm, is an essential element for the conversion of direct current (DC) to alternating current (AC) [17-18]. The modulation index of the Pulse Width Modulation (PWM) technique is utilized to determine the resulting output voltage of the inverter, once the voltage at the Direct Current (DC) bus has reached a stable condition. The control scheme utilizing Long Short-Term Memory (LSTM) Artificial Neural Network (ANN) controllers is depicted in Figure 5. Ensuring frequency stability is of utmost importance in a standalone system, as substantial deviations in active power imbalance can have adverse effects on the alternating current (AC) output frequency. The LSTM-ANN

controller utilizes the error signal of the frequency and its reference to calculate the reference component of the direct axis current. Applying a comparable methodology, the root mean square (RMS) voltage is compared to its reference value in order to generate the reactive signal of the current. The switches are controlled by signals generated using an SVPWM (Space Vector Pulse Width Modulation) technique, as illustrated in Figure 6.

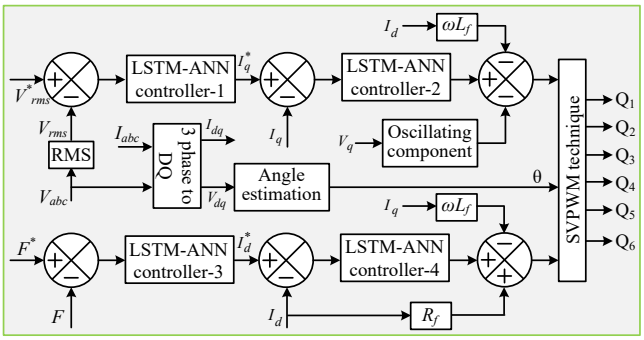

Figure 5: LSTM-ANN controller based proposed control scheme for inverter.

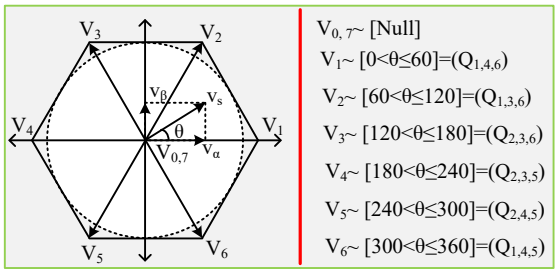

Figure 6: SVPWM Technique.

This research examines wind power generation systems that employ Permanent Magnet Synchronous Generator (PMSG) technology. It is crucial that each wind farm is equipped with a Point of Common Coupling (PCC) and a single inverter. Hence, it is crucial to establish a linkage between all Permanent Magnet Synchronous Generators (PMSGs) and a common Direct Current (DC) system, which is subsequently linked to the input of the respective inverter. Nevertheless, the direct integration of the output from all Permanent Magnet Synchronous Generators (PMSGs) is impractical because of the fluctuating wind speed. As a result, the electrical energy produced by each Permanent Magnet Synchronous Generator (PMSG) is first transformed into Direct Current (DC) through an uncontrolled rectifier before being integrated into the system. To serve as a Maximum Power Point Tracking (MPPT) circuit for the turbine, the boost converter depicted in Figure 1 is utilized in combination with a Sliding Mode Control (SMC) technique. The SMC (Sliding Mode Control) controller does not necessitate the need for wind turbine speed detection. The sliding mode controller (SMC) that has been implemented is illustrated in Figure 7. The specifications that have been used are provided in detail in Table-1.

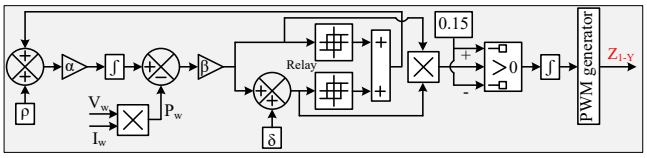

Figure 7: SMC-MPPT.

Table-1: Parameters of Figure 7.

S.No	Parameters	Values
1	α	127.
2	β	0.13.
3	ρ	0.89.
4	δ	0.96.

The boost converters of the wind farm are interconnected in parallel via a common DC-bus, enabling the transfer of power generated by all the Permanent Magnet Synchronous Generators (PMSGs) to the microgrid. This is accomplished by raising the DC-link voltage, even during periods of low wind speed. Moreover, these circuits have the capability to operate as Maximum Power Point Tracking (MPPT) devices for each individual wind turbine by employing Switched Mode Control (SMC). Each photovoltaic (PV) plant consists of multiple PV arrays, where each array is connected to its own maximum power point tracking (MPPT) converter. In order to optimize cost-efficiency and system efficiency, a single inverter is employed to establish a connection between the dc-link and the load. To enhance comprehension, please consult Figure 8(a) and (b), illustrating the block diagram of the Photovoltaic (PV) array under Partial Shading Conditions (PSCs) and the PV cell, respectively.

The photovoltaic (PV) string comprises 22 PV modules that are interconnected in a series configuration, resulting in an output voltage of 660V under maximum irradiance conditions. The technical specifications of a single photovoltaic (PV) module can be located in the Appendix section. To enhance the efficiency of Maximum Power Point Tracking (MPPT) converters, a cost-effective strategy is employed by parallelly connecting three photovoltaic (PV) strings to create each PV array. As a result, a single DC-DC circuit can efficiently operate as a Maximum Power Point Tracking (MPPT) circuit for the entire Photovoltaic (PV) array, which consists of three strings. However, this specific configuration is highly vulnerable to PSC (Potential Security Compromise). Therefore, it is imperative to design an MPPT (Maximum Power Point Tracking) algorithm that can effectively control the Perturb and Observe (P&O) technique and optimize power extraction across diverse operating conditions. The two distinct Power System Control (PSC) scenarios are outlined in Table-2 and are simulated using the models referenced in [1, 4].

Table-2: list of PSCs.

Pattern	Single PV string
1	[PSC-1]: **Figure 9(b).** Modules: 1–4=1000W/m^2, modules: 5–8=750W/m^2, modules: 9–18=610W/m^2, modules: 19–22=405W/m^2
2	[PSC-2]: **Figure 9(b).** Module: 1=1000W/m^2, modules: 2–5=820W/m^2, modules: 6–12=580W/m^2, modules: 13–22=395W/m^2

Regulating the photovoltaic (PV) system to function at a designated voltage level referred to as V_{mpp} is crucial for maximizing its power generation. This is illustrated in Figure 9(a) for different levels of irradiance. However, the conventional perturb and observe (P&O) algorithm encounters difficulties in precisely determining the maximum power point (MPP)

location in the presence of partial shading conditions (PSC), as depicted in Figure 9(b), because of the existence of multiple local maximum locations. Within the P&O technique, the perturbation direction is adjusted based on the polarity of the power change along the P-V curves. The voltage at the Maximum Power Point (MPP) is determined by equation (1). The user's input is a data structure known as a list, which is a collection of elements. In this case, the list contains the elements 1 and 4.

$$V_{\text{mpp}}(i) = \Delta V \times \text{sign}\left(\frac{dP_{\text{pv}}}{dV_{\text{pv}}}\right) + V_{\text{mpp}}(i-1) \qquad (7)$$

The delta voltage, ΔV, represents an incremental change, while the iteration number is denoted as 'i'.

Within the domain of Photovoltaic Solar Cells (PSC), it is a common phenomenon to observe the existence of multiple local peaks. However, it is feasible for one of these peaks to represent the GMPP (Global Maximum Power Point), as illustrated in Figure 9(b). Traditional Maximum Power Point Tracking (MPPT) techniques such as Perturb and Observe (P&O) and incremental impedance may not provide a dependable guarantee of achieving the Global Maximum Power Point (GMPP). Thus, the Perturb and Observe (P&O) algorithm is combined with the Modified Invasive Weed Optimization (MIWO) technique to accurately identify the Global Maximum Power Point (GMPP) while minimizing oscillation in Photovoltaic Solar Cells (PSCs). The locations of local and global maximum power points (MPPs) can experience random fluctuations caused by changes in shading conditions and the configuration of the photovoltaic (PV) module, as depicted in Figure 9(b).

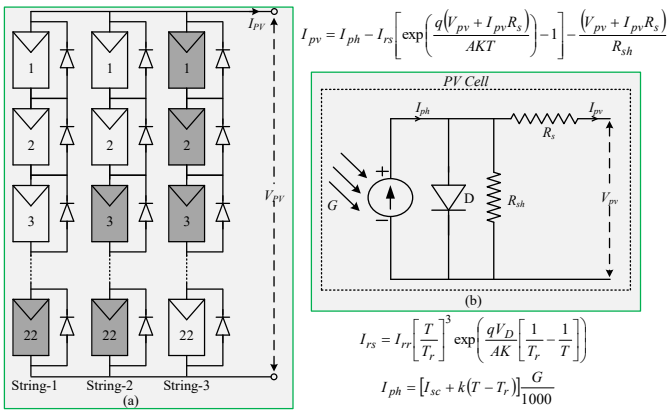

Figure 8: (a) PV Array, (b). PV Cell.

The aim of integrating the Pattern and Orientation (P&O) algorithm with the Multiple-Objective Improved Water Optimization (MIWO) algorithm is to enhance their respective capabilities and advantages. The prolonged response time of the MIWO technique can be attributed to the time it takes for the weeds to migrate towards the genetically modified pest population (GMPP). The strategy of this approach is to enable the spatial closeness of all the undesired vegetation to the GMPP (Genetically Modified Pest Plant). Upon the objects reaching a certain distance from each other, the P&O algorithm is initiated to enforce the Generalized Maximum Power Point (GMPP). If the absence of shading is not detected, the proposed process is executed utilizing the Perturb and Observe (P&O) method. However, if the Primary Synchronization Channel (PSC) is detected, the Maximum Likelihood Initial Timing Offset (MIWO) technique is utilized to locate the Global Maximum Power Point (GMPP). This is accomplished by continuously updating the Vmpp signal and adjusting the duty cycle of the respective Maximum Power Point Trackers (MPPTs), until the deviation in the optimal position of the weeds does not exceed 1.0%. The suggested Maximum Power Point Tracking (MPPT) methodology is illustrated in Figure 10 utilizing a flow chart.

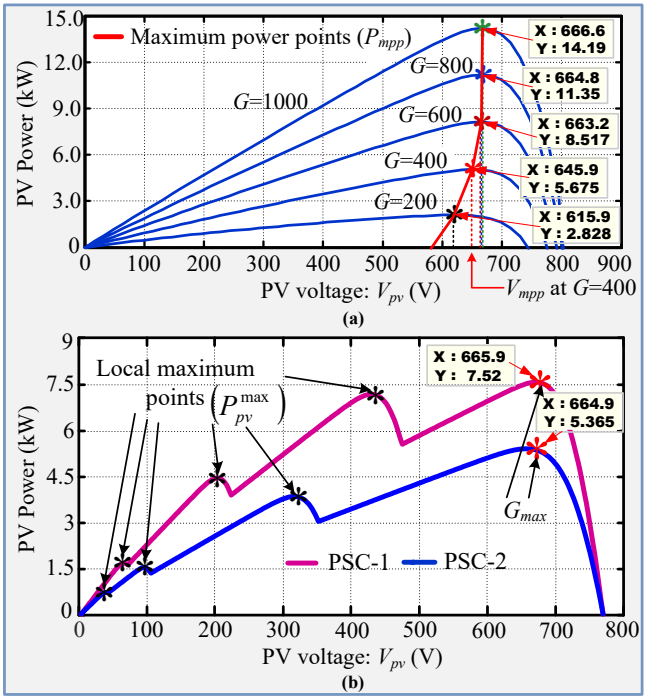

Figure 9: P-V characteristics (a) symmetrical irradiances, (b) PSCs.

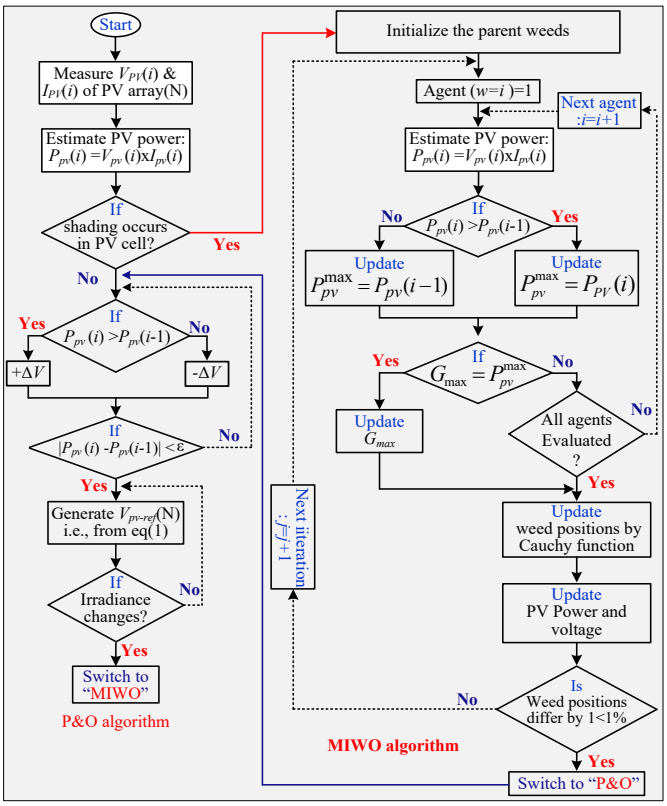

Figure 10: Proposed MIWO+P&O flow chart.

The P&O-MIWO algorithm is utilized to generate the reference voltage signal that corresponds to the Maximum Power Point (MPP). The input signal is subjected to a comparison operation with the voltage of the photovoltaic (PV) array using the Long Short-Term Memory-Artificial Neural Network (LSTM-ANN) controller, as illustrated in Figure 11. Each Maximum Power Point Tracking (MPPT) controller is purpose-built for its corresponding MPPT converter, such as the boost converter, which is situated within the Photovoltaic (PV) arrays, as depicted in Figure 1.

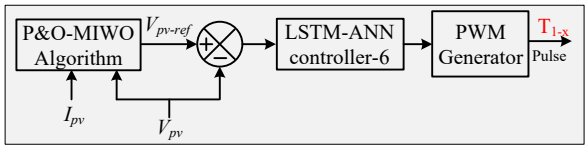

Figure 11: MPPT of PV units.

IV. Results and Discussions

Real-time simulators (RTS) equipped with sufficient computational power are capable of achieving performance levels that are comparable to real-time operations by accurately solving intricate power system equations, thereby effectively emulating the behavior of an authentic network.

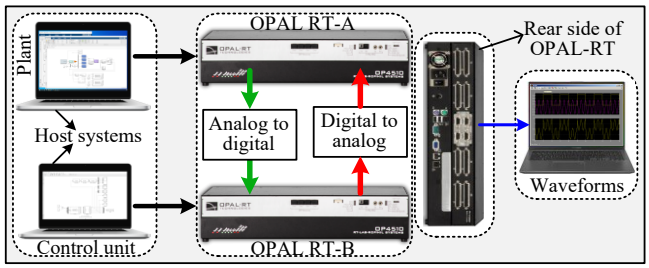

Figure 12: HIL setup.

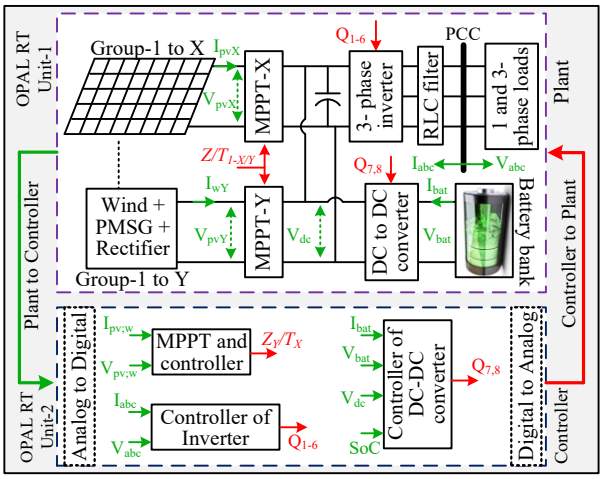

Figure 13: HIL implementation of proposed model.

To facilitate Hardware-in-Loop (HIL) testing, OPAL-RT technologies have designed and manufactured two Real-Time Simulation (RTS) units. The system, as illustrated in Figure 1, consists of two primary components: the plant, which encompasses all the physical elements, and the controlling unit, where all the controllers are situated. The initial module, Module-1, contains the plant model, while the second module is specifically designated for the controlling unit. Both units are equipped with digital and analog cables to facilitate the establishment of a loop. Analog signals will be transmitted from the plant to the control system via a continuous waveform, while digital signals will be transmitted from the control system to the plant using discrete binary values. An extensive analysis is performed on a distinct computer system to obtain comprehensive and detailed results. Figure 12 illustrates the arrangement of the Hardware-in-the-Loop (HIL) laboratory setup, displaying the interconnected cards that are of importance. Additionally, Figure 13 depicts a comprehensive block diagram of the Hardware-in-the-Loop (HIL) process of the proposed system, which includes the use of color coding.

Case-1: *performance under changes in generation and load*

The aggregate power output of all photovoltaic (PV) systems is aggregated to display a consolidated PV power output in the analysis. Similarly, the aggregate power generated by all wind systems is commonly known as wind power. Variations in the power outputs of photovoltaic (PV) and wind systems are depicted in Figure 14(a), in conjunction with fluctuations in the power consumption demanded by loads at the alternating current (AC) bus.

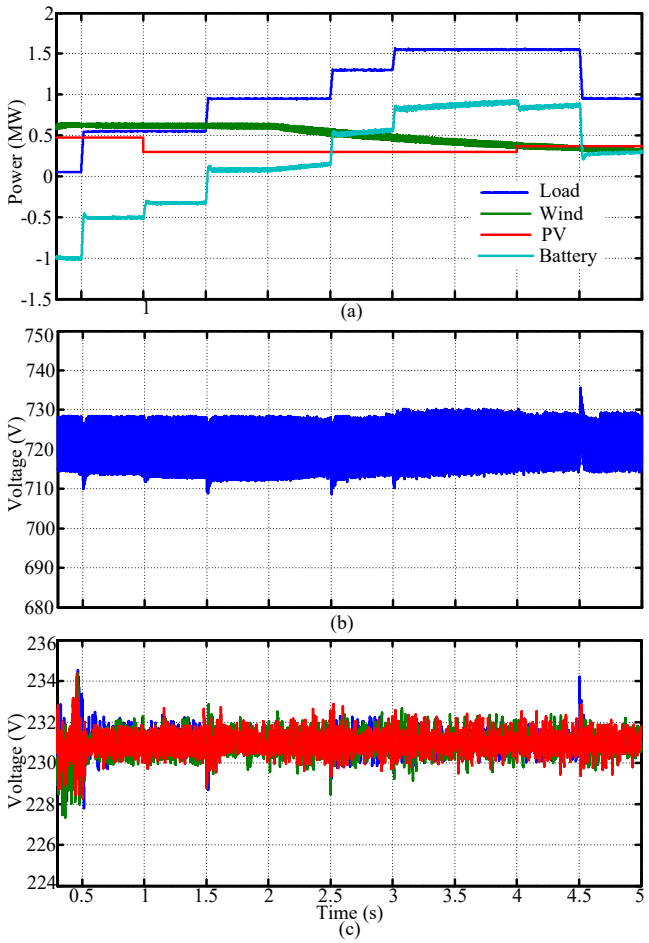

Figure 14: (a) Powers, (b) dc-link voltage, (c) RMS voltages.

In order to ensure power equilibrium within the system, the battery bank functions as a compensatory mechanism that rectifies any power disparities between the load and overall production. The charging process is characterized by the existence of negative power, while discharging is represented by positive power. This feature allows the battery to adjust for variations in the electrical load. The battery possesses the capability to regulate the voltage across the direct current (DC) terminals, known as the DC-link, as depicted in Figure 14(b). Notwithstanding voltage fluctuations induced by variations in load power, the magnitude of said fluctuations is negligible in comparison to the reference voltage of 720V. The root mean square (RMS) voltages of the three-phase system can be observed in Figure 14(c) under the specified conditions. The utilization of Long Short-Term Memory Artificial Neural Network (LSTM-ANN) control techniques results in consistent and reliable system responses. To achieve a more accurate assessment of the control techniques, the instantaneous load currents for the 3-phase system are illustrated in Figure 15.

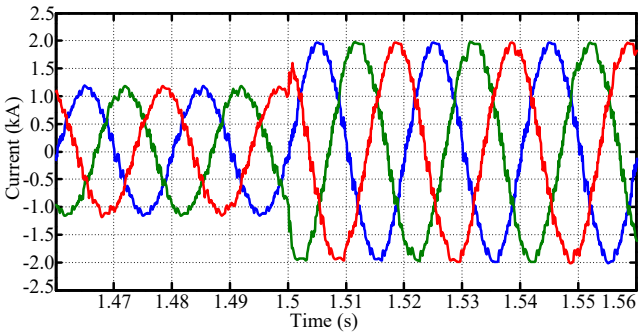

Figure 15: Instantaneous load bus currents.

Case-2: *performance under operation of unbalanced load.*

The predominant portion of loads operated in residential distribution systems are single phase, leading to an imbalanced load operation in a three-phase power supply system. The lack of equilibrium results in voltage imbalances that become apparent at the alternating current (AC) bus. Within the specified context, we are analyzing the characteristics of a three-phase unbalanced load, as depicted in Figure 16(a). In order to assess the efficacy of the proposed inverter controller, we are conducting an analysis on the load profile's worst-case scenario. The main objective of the proposed control system is to maintain and stabilize the amplitude and phase of the three-phase voltages at the load bus, thereby improving the power quality of the supplied electrical energy. The root mean square (RMS) voltages of the alternating current (AC) bus can be observed in Figure 16(b). During instances of abrupt changes at the load bus, there are minor fluctuations observed in the load current. Nevertheless, these variations ultimately converge to an equilibrium state at the reference voltage of 231V.

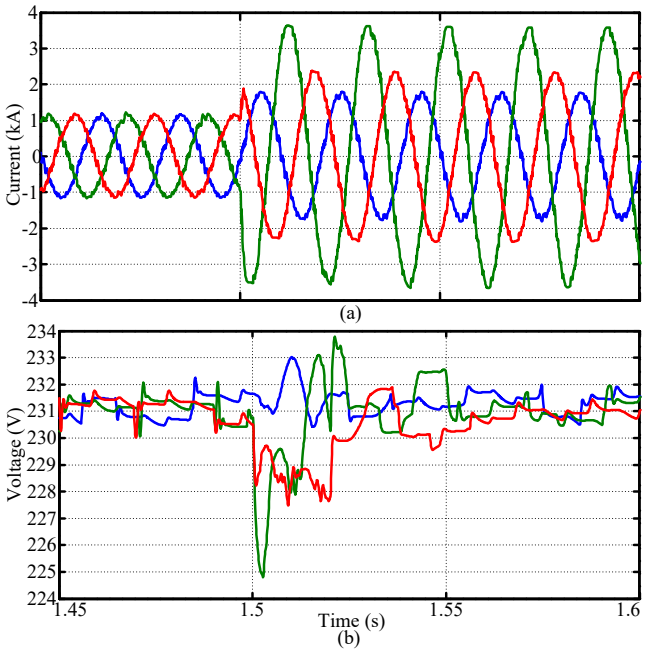

Figure 16: (a) current in unbalanced, (b) balanced RMS-phase voltages.

Case-3: PV-MPPT operation

In this scenario, the photovoltaic (PV) array consists of a singular array comprising three PV strings. The photovoltaic (PV) array is being tested under conditions of uniform

irradiance and potential-induced degradation (PID) caused by potential-induced degradation (PSC). Initially, the uniform irradiance is set to a value of 1000W/m2 and then decreases to 900W/m2 at a time of t=0.6s. The responses can be visually analyzed by referring to the provided graphical representation in Figure 17. The direct current (DC) link voltage of interest, represented as Vdc*(V_{mpp}), is depicted in Figure 17(b). The V_{mpp} (maximum power point voltage) is calculated through the utilization of MPPT (maximum power point tracking) algorithms that have undergone meticulous monitoring, as outlined in the preceding section. Following the reduction in irradiance at time t=0.60s, the reference signal experiences a minor decrease due to the precise tracking of the proposed Maximum Incremental Weighted Optimization and Perturb & Observe technique, as shown in Figure 17(b). In order to assess the efficacy of the suggested hybrid approach, an examination was conducted on the performance of the Maximum Power Point Tracking (MPPT) algorithm in comparison to two alternative optimization techniques: 1) Grey Wolf Optimization (GWO) [1], and 2) Particle Swarm Optimization (PSO) [1]. Figure 17 depicts the performance of the MIWO-P&O algorithm, which is the recommended method, in terms of enhancing the dynamic response of V_{mpp}. This algorithm demonstrates reduced oscillations and faster tracking compared to the other two optimization methods.

Figure 17(c) depicts the electrical output produced by a single array in the solar facility. The diagram depicts the effectiveness of the proposed Maximum Incremental Power Output - Perturb and Observe (MIWO-P&O) technique in improving the power extraction from the photovoltaic (PV) system. This enhancement is accomplished by generating an accurate reference signal. The DC voltage of the inverter used in the solar installation is shown in Figure 17(d). There is a small decrease in the DC-link voltage caused by changes in irradiance, but it stays within the designated range.

The performance evaluation of the Maximum Power Point Tracking (MPPT) algorithm, specifically the Modified Incremental Conductance (MIWO+P&O) algorithm, is conducted using Photovoltaic Solar Cells (PSCs) as outlined in Table 2. The electrical output produced by the photovoltaic (PV) system is illustrated in Figure 18(a). According to the analysis, it is evident that the proposed approach demonstrates superior performance in harnessing energy from the photovoltaic (PV) unit in comparison to the Grey Wolf Optimizer (GWO) and Particle Swarm Optimization (PSO) algorithms. Figure 18(b) depicts the Maximum Power Point (MPP) and the durations of tracking for Photovoltaic (PV) powers. The hybrid proposed method exhibits a time efficiency of 57% compared to Particle Swarm Optimization (PSO) in Problem Set C-1 (PSC-1) for tracking. Moreover, the proposed algorithm demonstrates the capability to extract a slightly higher power output in both PSC-1 and PSC-2. The results suggest that the algorithm being proposed exhibits superior performance in PSCs.

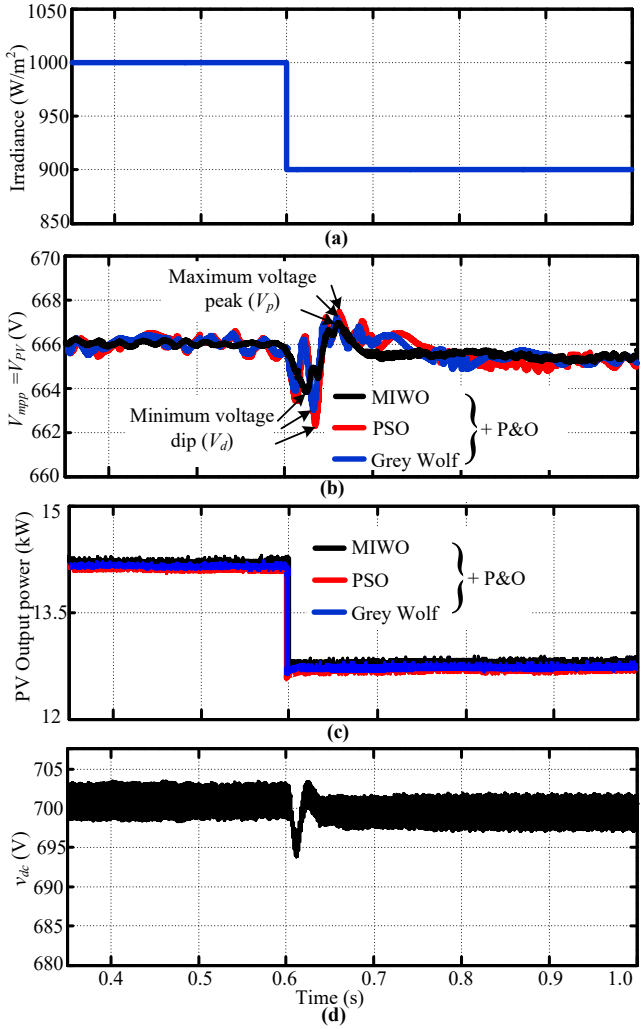

Figure17: (a) irradiance, (b) V_{mpp}, (c) Power from PV unit, (d) dc-voltage.

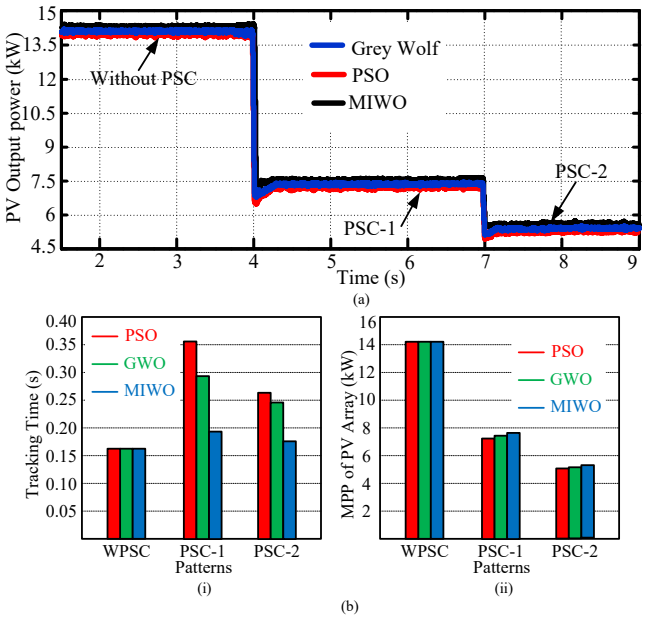

Figure 18: (a) PV powers, (b)-(i) Tracking performance, (b)-(ii) MPP.

Case-4: MPPT Performance of Wind Turbine

An alternative method for achieving accurate results from

Maximum Power Point Tracking (MPPT) involves the creation of a two-mass wind turbine model. The present model incorporates variations in wind velocity, specifically a transition from 12 to 7m/s at t=1.5sec, followed by a rise from 7m/s to 10m/s at t=4sec, as depicted in Figure 19. During the process of these modifications, the torque of the wind turbine is adjusted to match the reference torque. The reference torque is determined using wind turbine data obtained from sources [1, 3]. Figure 19 illustrates the relationship between the mechanical torque and the reference torque of the wind turbine. By employing a two-mass model, the torque undergoes a gradual reduction in response to an abrupt decrease in wind speed. According to the data depicted in Figure 19, it is evident that the turbine is functioning at its peak power output, as indicated by references [1, 3]. The torque of the Permanent Magnet Synchronous Generator (PMSG) is regulated by the current of the boost converter, ensuring that it accurately follows the desired torque as indicated by the reference torque.

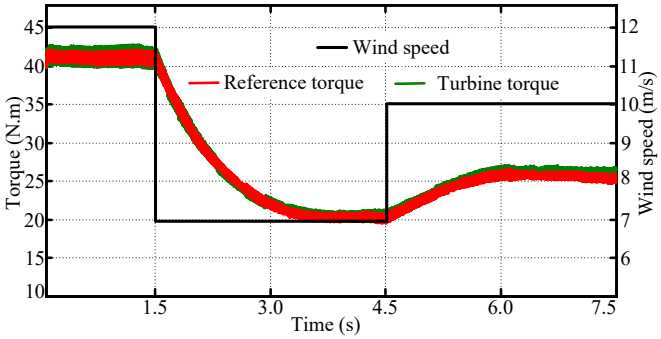

Figure 19: SMC-MPPT.

V. CONCLUSION

LSTM-based artificial neural network (ANN) controllers have been designed to regulate direct current (DC) to direct current (DC) circuits and inverters in standalone power supply models powered by hybrid renewable energy sources. The battery controller is a dedicated device designed to regulate power distribution between the total power generation and power consumption, ensuring a balanced equilibrium. A novel inverter control algorithm has been devised to maintain a stable voltage at the alternating current (AC) bus despite various factors such as load fluctuations, variations in solar irradiance, and changes in wind speed. The wind system, photovoltaic (PV) panels, and battery are integrated in a synergistic manner to ensure a reliable and stable power supply at the load bus. In order to evaluate the effectiveness of the suggested control techniques, a Hardware-in-the-Loop (HIL) simulation is performed utilizing OPAL-RT units. The proposed inverter control technique allows for the maintenance of balanced three-phase voltages at the load terminal, even in the presence of unbalanced load conditions. The power quality is significantly enhanced through the utilization of advanced control strategies on both the direct current to direct current circuit and the inverter, leading to optimal performance in all operational scenarios.

Appendix:

Parameters of 0.5MW PV system.

215.0W module		
S.No	Parameter(s)	Rating
1	Current when short-circuit.	8.01A
2	Open-circuit terminal voltage.	36.9V
3	Voltage at MPP (V_{mpp}).	30.3V
4	Current at V_{mpp}.	7.10A
Combinations for Series and parallel of 0.5MW		
5	'N' in String.	21
6	'M' in Group.	7
7	'X' in PV System.	16

Parameters of Single wind-PMSG system [19-20].

Parameters of a Two Mass Drive Train

H_t	4.0s.
H_g	$0.11H_t$.
K_{sh}	0.32p.u./el.rads.
D_t	0.71p.u.s/el.rads.

Parameters of PMSG

Pole pairs	5.0
Operating speed	153.4rad/s.
Magnetic flux linkage	0.432Wb.
Stator inductance (L_s)	8.41mH.
Armature resistance (R_s)	0.424Ω.
Rated torque	40.0Nm.
Operating power	6.41kW.

Ratings of batteries.

The battery ratings are determined through a comprehensive analysis of the appropriate voltage and power parameters. In this section, a basic example is provided, along with numerical calculations, to clarify this specific concept. The primary factor that determines the battery rating is the duration of discharge. The aim of this study is to develop a battery bank with a voltage rating of 480.0V that can function as a backup power supply for a period of 72.0 hours. The battery bank will have the capacity to support a steady load of 0.5 megawatts at the point of common coupling (PCC). The calculation of the current rating (Ah) of the batteries is determined using the given expression, assuming a state of charge (SoC) of 0.6.

$$I_{bat} = \frac{5{,}00{,}000 \times 72}{0.6 \times 480} = 125\,kAh$$

Parameters of a batteries.

125kAh-400V ratings of battery bank.		
S.No	Parameters	Ratings
1	Single battery voltage.	48V
2	Single battery current rating.	125A
3	Number of batteries per string (series).	10.0
4	Required parallel strings.	1000

References

[1]. Siva Ganesh Malla, et al., "Coordinated Power Management and Control of Renewable Energy Sources based Smart Grid",

International Journal of Emerging Electric Power Systems, **early access**, https://doi.org/10.1515/ijeeps-2021-0113

[2]. A. Dash, et al., "DC-Offset Compensation for Three-Phase Grid-Tied SPV-DSTATCOM Under Partial Shading Condition With Improved PR Controller," *IEEE Access*, vol. 9, 2021, doi: 10.1109/ACCESS.2021.3115122.

[3]. H. U. R. Habib et al., "Optimal Planning and EMS Design of PV Based Standalone Rural Microgrids", *IEEE Access*, vol. 9, 2021, doi: 10.1109/ACCESS.2021.3060031.

[4]. C. Pradhan, et. al., "Coordinated Power Management and Control of Standalone PV-Hybrid System With Modified IWO-Based MPPT", *IEEE Systems Journal*, vol. 15, no. 3, pp. 3585-96, Sept. 2021, doi: 10.1109/JSYST.2020.3020275.

[5]. D. Bhule, S. Jain and S. Ghosh, "Control Strategy for Photovoltaic-Battery Based Standalone System", *IEEE First International Conference on Smart Technologies for Power, Energy and Control (STPEC)*, 2020, pp. 1-6, doi: 10.1109/STPEC49749.2020.9297685.

[6]. S. G. Malla, C. N. Bhende and S. Mishra, "Photovoltaic based water pumping system", *International Conference on Energy, Automation and Signal*, 2011, pp. 1-4, doi: 10.1109/ICEAS.2011.6147148.

[7]. S.G. Malla, C.N. Bhende, "Voltage control of stand-alone wind and solar energy system", *International Journal of Electrical Power & Energy Systems*, Volume 56, 2014, Pages 361-373, https://doi.org/10.1016/j.ijepes.2013.11.030.

[8]. S.G. Malla, C.N. Bhende, "Enhanced operation of stand-alone "Photovoltaic-Diesel Generator-Battery" system", *Electric Power Systems Research*, Volume 107, Pages 250-257, 2014, https://doi.org/10.1016/j.epsr.2013.10.009.

[9]. Malla, Priyanka, Malla, Siva Ganesh and Calay, Rajnish Kaur. "Voltage control of standalone photovoltaic – electrolyzer- fuel cell-battery energy system" *International Journal of Emerging Electric Power Systems*, 2022. https://doi.org/10.1515/ijeeps-2022-0047

[10]. R. D. Bhagiya and R. M. Patel, "PWM based Double loop PI Control of a Bidirectional DC-DC Converter in a Standalone PV/Battery DC Power System", *IEEE 16th India Council International Conference (INDICON)*, 2019, pp. 1-4, doi: 10.1109/INDICON47234.2019.9028974.

[11]. Manisha, M. M. Masoom and N. Kumar, "Comparative Study of Nonlinear Controllers for Standalone PV System", *Second International Conference on Electronics and Sustainable Communication Systems (ICESC)*, 2021, pp. 25-31, doi: 10.1109/ICESC51422.2021.9532701.

[12]. U. R. Muduli and K. Ragavan, "Dynamic modeling and control of shunt active power filter," 2014 Eighteenth National Power Systems Conference (NPSC), 2014, pp. 1-6, doi: 10.1109/NPSC.2014.7103893.

[16]. A. Dash, et.al, "Performance Evaluation of Three-Phase Grid-tied SPV-DSTATCOM with DC-offset Compensation Under Dynamic Load Condition", *IEEE Access*, doi: 10.1109/ACCESS.2021.3132549.

[17]. V. Narayanan, S. Kewat and B. Singh, "Solar PV-BES Based Microgrid System With Multifunctional VSC", *IEEE Transactions on Industry Applications*, Vol. 56, no. 3, pp. 2957-2967, May-June 2020, doi: 10.1109/TIA.2020.2979151.

[18]. X. Song, Y. Zhao, J. Zhou and Z. Weng, "Reliability Varying Characteristics of PV-ESS-Based Standalone Microgrid", *IEEE Access*, Vol. 7, pp. 120872-120883, 2019, doi: 10.1109/ACCESS.2019.2937623.

[19]. Koilada Rajesh, "Novel Control of Boost Converter for MPPT of Wind Turbine", International Journal of New Technologies in Science and Engineering (IJNTSE), Vol. 8, Issue. 6, pp. 1-6, June. 2022.

[20]. O N Chandrasekhar, "Modified Sliding Mode Control for MPPT of PMSG based Wind Power Generation System", International Journal of New Technologies in Science and Engineering (IJNTSE), Vol. 8, Issue. 8, pp. 8-13, Aug. 2022.

[21]. U. R. Muduli, et al., "Cell Balancing of Li-ion Battery Pack with Adaptive Generalised Extended State Observers for Electric Vehicle Applications", *IEEE Energy Conversion Congress and Exposition (ECCE)*, 2021, pp. 143-147, doi: 10.1109/ECCE47101.2021.9595601.